مجلة ابن الهيثم للعلوم الصرفة والتطبيقية المجلد 23 (3) 2010

تحقيق نظري لتحسن قوام الكسب الكهروحراري للتراكيب المنخفضة الابعاد

محمود راضي جبير، إبتسام محمد تقي سلمان* ، أيسر صباح كيتب

قسم الأشعة ، كلية التقنيات الصحية والطبية

***قسم الفيزياء ،كلية التربية– ابن الهيثم ، جامعة بغداد**

الخلاصة

إن معاملاتَ القدرة والتوصيلات الحرارية الإلكترونية في البزموث–تليورايد (Bi_2Te_3) والليد–تليورايد (PbTe) والكاليوم–ارسنايد (GaAs) في درجةِ حرارة الغرفةِ (300 كلفن) في حالة أسلاك كمية وآبار كمية حققت نظرياً. الصيغ المستخدمة هنا تأخذ في الحسبان بدقة شديدة تعديل معاملاتِ القدرة والتوصيلاتِ الحراريةِ الإلكترونيةِ في الأسلاكِ والآبارِ الكميةِ ذي السطوح الحرة بسبب الاحتجاز المكاني. من نتائجنا العدديةِ، نتوقعُ زيادة مهمة في معاملِ القدرة للأسلاكِ الكميةِ بالقطرِ 20Å . إن الزيادةَ أقوى دائماً في الأسلاكِ الكميةِ من الآبارِ الكميةِ ذي الأبعادِ المطابقةِ. إفترضَ التوزيعُ الفونوني غير مقيد مستند الى التوصيلِية الحرارية الشبكية الحجميةَ ثمّ إستخدمَ لتَقييم التحسنِ المحتملِ لقوام الكسب. التوصيل الحراري الإلكتروني لسلك بقطر 20Å وطبقةِ بسمك 20Å تَبَيَّن انه كَانَ لَيسَ نقصاناً مهمّاً. قوام الكسب الناتج، المحسوبَ لـ Bi_2Te_3 و PbTe و GaAs، في حالة أسلاك كمية وآبار كمية، اظهر زيادَة بشكل ملحوظ. إنّ تحسينَ قوام الكسب الكهروحراري الإضافي في الغالب بسبب احتجازِ الناقلِ في بعدين وفي بعد واحد الذي يُؤدّي إلى تحسينِ معاملِ القدرة.

IBN AL- HAITHAM J. FOR PURE & APPL. SCI. VOL.23 (3) 2010

A Theoretical Investigation of Enhanced Thermoelectric Figure of Merit of Low-Dimensional Structures

M. R. Jubayr, E. M-T. Salman* ,A. S. Kiteb
Foundation of Technical Education,College of Medical Technology
*** Department of Physics, College of Education Ibn Al-Haitham ,University of Baghdad**

Abstract

The power factors and electronic thermal conductivities in bismuth telluride (Bi_2Te_3), lead-telluride (PbTe), and gallium arsenide (GaAs) at room temperature (300K) quantum wires and quantum wells are theoretically investigated. Our formalism rigorously takes into account modification of these power factors and electronic thermal conductivities in free-surface wires and wells due to spatial confinement. From our numerical results, we predict a significant increase of the power factor in quantum wires with diameter w=20 Å. The increase is always stronger in quantum wires than in quantum wells of the corresponding dimensions. An unconfined phonon distribution assumed based on the bulk lattice thermal conductivity is then employed to evaluate the possible enhancement of the thermoelectric figure of merit. The electronic thermal conductivity of a 20Å diameter wire and a 20Å layer thickness is found to be of no significant decrease. The resultant ZT, calculated for Bi_2Te_3, PbTe and GaAs, quantum wires and quantum wells, showed increase significantly. The additional thermoelectric figure of merit enhancement is mostly due to the two- and one-dimensional carrier confinement which lead to the enhancement of power factor.

Introduction

Direct conversion of thermal energy to electrical power and in solid-state cooling is a promising method for many applications [1,2]. Often, these applications require reliable and durable materials that require little or no maintenance for years on end. Examples include deep space probes and heat regulators for computer processors. Thermoelectric (TE) materials fit these requirements extremely well by using the Seebeck and Peltier cooling effects. But TE devices are still not a commercially-viable alternative to conventional generators and coolers because the energy conversion efficiencies of these devices remain generally poor [2,3]. In recent years these devices have witnessed a strong renewal of interest with the proposals to improve the electric properties of some materials [4]. However, most present research into thermoelectrics deals with developing compounds and devices that have greater efficiency [5-7].

The energy conversion efficiency of a material is limited by the dimensionless quantity ZT, where T is the absolute temperature and Z is the thermoelectric figure of merit: defined as $Z=S^2\sigma/\kappa$, where S is the thermoelectric power or Seebeck coefficient, σ is the electrical conductivity, and κ is the total thermal conductivity [1,2,8]. Further, κ is the sum of the

electronic part κ_e and of the lattice part κ_p, $\kappa = \kappa_e + \kappa_p$ [9,10,11]. Clearly, high ZT requires high S, high σ, and low κ for maximum conversion of heat to electrical power or electrical power to cooling. Since the three parameters defining the thermoelectric figure of merit ZT are

in most cases interdependent, i.e. as an increase in S implies a decrease in σ, and an increase in σ implies an increase in the electronic contribution to κ [3,12,13].

In spite of an enormous effort by a huge number of scientists and a large number of publications in this area, the highest value of the three dimensional (3-D) bulk thermoelectric figure of merit ZT at room temperature T remains ZT≈1 (8). It is believed that if materials with ZT≥3 (corresponds to about 20-30% Carnot efficiency) could be developed, many more practical applications for thermoelectric devices would see the light such as laser diodes, infrared detectors, microprocessors, blood analyzers, portable picnic coolers as well as many other applications in aerospace [3,11,14]. Nowadays Peltier refrigerators are mainly used in situations in which reliability and quiet operation (but not the cost and conversion efficiency is the main concern), like equipments in medical applications, space probes etc. [15].

The use of low-dimensional materials systems, as realized in the form of two-dimensional (2-D quantum wells) nanostructures and one-dimensional (1-D quantum wires) nanostructures has been shown to provide a promising strategy for increasing ZT relative to bulk values [16]. The interest in low-dimensional structures for thermoelectric applications was motivated by the increase in carrier density of states per unit volume with shrinking device dimensions while the thermal conductivity can be decreased due to confinement effects [17,18]. Electron confinement in low-dimensional structures leads to a radical change in physical properties of these systems as compared with bulk crystals and, in principle, introduces new opportunities to vary S, σ, and κ independently [13,19].

In the present paper the power factor of *n*-type (Bi_2Te_3, PbTe and GaAs) and the electronic thermal conductivity are investigated in the frames of the quantum well and quantum wire models taking into account spatial confinement of electrons only. The materials systems are chosen for numerical simulation because of their great greeter promise for high temperature thermoelectric applications [20].

Theoretical modeling

The general expressions of S, σ, κ_e for bulk, quantum well, and quantum wire materials were modeled using Boltzmann transport equation (BTE) and constant relaxation-time approximation, $\langle\tau\rangle$, and that of parabolic bands [14]. To obtain explicit results for ZT, one of three approachescan be used which are discussed in Ref.[19]. However, we do assume that the carrier mobility coincides with the bulk value and the approach used here is as follows: κ_p is conservatively approximated using 3-D bulk experimental data; this assumption does not severely restrict the analysis. The thermoelectric parameters for confined electrons in a (1-D, 2-D and 3-D) structures are given in Ref. [11,14,20-23].

i. 3D Model

$$\sigma^{3D} = \frac{e^2}{3\pi^2}\left(\frac{2k_BT}{\hbar^2}\right)^{3/2}(m^*)^{3/2}\mu_x(3F_{1/2}/2) \qquad (1)$$

where $m^* = (m_x m_y m_z)^{1/3} = (m_t^2 m_l)^{1/3}$ is the effective density of states mass of electrons in the band, e is the electron charge, k_B is the Boltzmann's constant, $\hbar$ is the Plank constant divided by

2π,□□$_x$ is the carrier mobility ($\langle\tau\rangle e/m_x$) in the x direction (i.e. 100 direction), and F_i is the Fermi–Dirac integral defined as

$$F_i = F_i(\xi^*) = \int_0^\infty \frac{x^i dx}{\exp(x - \xi^*) + 1} \quad (2)$$

$\xi^* = \xi / k_B T$ is the reduced chemical potential (relative to the edge of the conduction band). Also, the electric conductivity can be expressed as,

$$\sigma = |e| \mu_e n_e \quad (3)$$

where n_e is the electron density.

$$S^{3D} = -\frac{k_B}{e}\left(5F_{3/2}/3F_{1/2} - \xi^*\right) \quad (4)$$

$$K_e^{3D} = \frac{k_B^2 T}{3\pi^2 e}\left(\frac{2k_B T}{\hbar^2}\right)^{3/2} (m^*)^{3/2} \mu_e \left(7F_{3/2}/2 - 25F_{3/2}^2/9F_{1/2}\right) \quad (5)$$

In low-dimensional structures, these expressions must be reformulated.

ii. 2D Model

In early models for thermoelectricity in 2-D quantum well and 1-D quantum wire structures it was again assumed that the electrons in the valence and conduction bands are in simple parabolic energy bands and that the electrons occupy only the lowest subband (complete quantum confinement) of the quantum well or quantum wire.

$$\sigma^{2D} = \frac{\langle\tau\rangle e^2}{2\pi w}\left(\frac{2k_B T}{\hbar^2}\right)(m_y/m_x)^{1/2} F_0 \quad (8)$$

$$S^{2D} = -\frac{k_B}{e}\left(2F_1/F_0 - \xi_{2D}^*\right) \quad (9)$$

$$K_e^{2D} = \frac{\langle\tau\rangle k_B \hbar^2}{4\pi w}\left(\frac{2k_B T}{\hbar^2}\right)^2 (m_y/m_x)^{1/2}\left(3F_2 - 4F_2^2/F_0\right) \quad (10)$$

where w is the width of the quantum well (layer thickness).

iii. 1D Model

It is further assumed that the quantum confinement is in the z direction. Let us consider a quantum wire of circular cross-section that has a radius w and an infinite length along the x-axis. Solutions of Boltzmann's equation were then obtained for S, σ, and κ_e for 1-D system.

$$\sigma^{1D} = \frac{\langle\tau\rangle e^2}{\pi w^2}\left(\frac{2k_B T}{\hbar^2}\right)^{1/2} (1/m_x)^{1/2} F_{-1/2} \quad (14)$$

$$S^{1D} = -\frac{k_B}{e}\left(3F_{1/2}/F_{-1/2} - \xi^*\right) \quad (15)$$

$$K_e^{1D} = \frac{4k_B^2 T\langle\tau\rangle}{\pi w^2}\left(\frac{2k_B T}{\hbar^2}\right)^{1/2} (1/m_x)^{1/2}\left(5F_{3/2}/2 - 9F_{1/2}^2/2F_{-1/2}\right) \quad (16)$$

Results and Discussion

The power factor (*PF*) of a bulk and reduced dimensions (1-D and 2-D) is investigated herein for illustration using the band parameters listed in Table 1. To obtain the maximum power factor

(PF_{max}), we use the equations (1, 4, 8-9, 14-15) subjected to the free-surface boundaries conditions. The Seebeck squared coefficient (S^2) obtained for each material system is the product by that value of the electric conductivity (σ) to obtain the power factor PF. The power factor characteristics were calculated for the three material systems (Bi_2Te_3, PbTe and GaAs). In Fig.1 we show the PF curves of the testing materials for various concentration (doping) levels which was calculated by applying a constant temperature at 300K while changing the carrier concentration between $10^{16}cm^{-3}$ and $10^{20}cm^{-3}$ using the MatLab Software.

It is evident from Fig.1 that the PF increase with reducing the dimension of the material, (wire system), has higher value for all materials and the best material is GaAs (see Fig.2). This increase is due mainly to the enhancement of the density of electronic states per unit volume that occurs for small widths. Several interesting phenomena are observed in Fig.1 the PF at low concentration ($10^{16}cm^{-3}$) and higher concentration ($10^{20}cm^{-3}$) conditions approaches to zero for all material in the three models (1-D, 2-D and 3-D). The very high electron confinement in the wire led to PF contribution only from states around the conduction band edge. In the case of low carrier concentration, the conduction band edges and the subsequent subband energy levels are located at a few eV above the Fermi level as seen in Fig.3. For example, for a concentration of $5\times10^{16}cm^{-3}$, the value of the Fermi Level of GaAs is 0.1eV below the conduction band edge. Also, as seen in Fig.3, high concentration brings the conduction band edge closer to the Fermi level. The variation of PF with Fermi Level is shown as in inset in Feg.3. The maximum value of PF_{max} occurs when the conduction band edge is closer to the Fermi level. As the *n* increases, the σ increases and are also causing the increase of κ_e. In reality, as the carrier concentration of all cases increases and the PF is expected to reach a maximum before starting to reduce with an increase in carrier concentration due to interdependency of the electronic conductivity σ and Seebeck coefficient S, that is, at the certain values of σ and S, the PF has maximum value. As it was already mentioned, the lattice thermal conductivity of low-dimensions κ_p will be taken the same as in bulk.

In calculations we assumed $w = 20\text{Å}$ free-surface boundaries wire and well. It was found that for $n \approx 10^{19}cm^{-3}$ the expected values of the maximum power factor for (Bi_2Te_3), (PbTe) and (GaAs) are $PF=67\mu W/cmK^2$, $PF=96\mu W/cmK^2$, and $PF=382\mu W/cmK^2$ which are, respectively, 8, 12 and 13 times higher than the measured value in their bulk structures, at these values the κ_e values are (Bi_2Te_3: 1.9387W/m-K), (GaAs: 6.9303W/m-K) and (PbTe: 2.0560 W/m-K).

Fig.4 shows the electronic thermal conductivity values as a function of doping for 20Å obtained using the eqs.(3, 5, 10, 16). When the dimensions is reduced from 2-D to 1-D electron confinement are increased from 1-D to 2-D. Calculations for electronic thermal conductivity indicate that 1-D with very small wire diameter (20Å) as in the case of the GaAs wire causing a 6% increasing in electronic thermal conductivity (from 7.0934W/m-K in 3-D bulk to 7.5172W/m-K in 1-D at concentration about $10^{-3}cm^{-3}$). Although different structures lead to significant difference in the PF between them, the slope of electronic thermal conductivity of each bulk, well and wire structures is very close in all cases and always higher that in the wire. That is κ_e rises slightly above the bulk value in situation 1-D while the situation for 2-D in a quantum well is, however, quite different because κ_e is slightly reducued 9% (6.4699 W/m-K) below the bulk value (see inset Fig. 4).

Accordingly, the results for both structures (1-D and 2-D) show a significant increase in ZT as the quantum well and wire dimensions are lowered. For the considered value of *w* in the

present work, ZT for the quantum wire is higher than for the quantum well. Most this additional enhancement comes from the increase of PF only while the slight increase in κ_e has little negative effect on it.

It is evident from the results above that Z2DT and Z1DT increase substantially above the bulk value for the decreasing dimensions of well and wire. This is a consequence of the increased effects of carriers (electrons) confinements that occur as the well and wire dimensions decrease. For the thickness considered (20Å), the wire has PF compared to the bulk leading to a factor of 6.5 increases in the ZT of the Bi_2Te_3 wire while 3 of the PbTe and 28 of the GaAs (see Table 2). The resultant GaAs ZT calculated with quantum wire structure is Z1DT=0.2397 at 300 K, which is rather small, although much larger than the corresponding Z3DT for bulk GaAs (Z3DT=0.0085 at 300 K).

Conclusion

We have theoretically investigated the figures of merit for quantum well and quantum wire structures which are compared to reveal the size confinement effects on enhanced thermoelectric figure of merit. The size confinement effects on the thermoelectric power factors, the electronic thermal conductivity, and the position of Fermi level are all examined and discussed. The dependence of the thermoelectric power factors and electronic thermal conductivity on carrier density is calculated and optimal parameters are determined. The quantum well thermoelectric figure of merit Z2DT as a function of well width is studied for quantum well and quantum wire structures with different carrier densities. It is found that Z2DT increases with decreasing well width and this increase is more pronounced in quantum wire structures. The computational results show that the figure of merit is 6.5 times higher than that in bulk Bi_2Te_3, 3 times higher than that in bulk PbTe and 28 times higher than that in bulk GaAs because of an increase in their power factor with increasing spatial confinement. Electronic thermal conductivity has little effect (negatively or positively) in the situation 1-D and 2-D on ZT.

References

1. Chen,G.;Narayanaswamy,A. and Dames,C. (2004) Engineering nanoscale phonon and photon transport for direct energy conversion, superlattices and Microstructures, 35:161–172.
2. Medlin,D.L.and Burns,A. (2009) Experiment and theory are providing new insights in nanostructured thermoelectric alloys, SAND, P. 1131.
3. Ramayya,E.B.and Knezevic,I. (2009) ,Ultrascaled Silicon Nanowires as Efficient Thermoelectric Materials, Pro. 13th IWCE, IEEE.
4. Sur,I.; Casian,A.and Balandin,A. (2004) Electronic thermal conductivity and thermoelectric figure of merit of *n*-type PbTe/$Pb_{1-x}Eu_xTe$ quantum wells, Phys. Rev. B 69, pp. 1-7.
5. Snyder,G.J.; Stephens,P.W.and Haile,S.M. (2005) Synchrotron X-ray structure refinement of Zn_4Sb_3, Int. Conf. Thermoelectrics, IEEE, p. 312.
6. Ikeda,T.; Azizgolshani,H.; Haile,S.M.; Snyder,G.J.and Ravi,V.A. (2005)Solidification Processing of Te–Sb–Pb Alloys For Thermoelectric Applications, Int. Conf. Thermoelectrics, IEEE, p. 132.

7. Ikeda,T.; Ravi,V.; Collins,L.A.; Haile,S.M. and Snyder,G.J. (2006) Development of Nanostructures in Thermoelectric Pb-Te-Sb Alloys, Int. Conf. Thermoelectrics, IEEE, pp. 1-4244-081.
8. Vashaee,D.and Shakouri,A. (2004) Improved Thermoelectric Power Factor in Metal-Based Superlattices, Phys. Rev. Lett. 92 (10): 1-4.

9. Huang,M.J.; Chang,T.M.; Chong,W.Y.; Liu,C.K. and Yu,C.K. (2007) A new lattice thermal conductivity model of a thin-film semiconductor, Int. J. Heat Mass Transfer, 50, 67–74.
10. Xu,G.; Chen,T.; Liu,J.and Zhou,Z. (2003) Thermoelectric properties of porous $(Bi_{0.15}Sb_{0.85})_2Te_3$ thermoelectric materials, J. University of Science and Technology Beijing, 10 (5): 39-43.
11. Casian,A.; Dashevsky,Z.; Kantser,V.; Scherrer,H.and Sur,I. (2002) Thermoelectric figure of merit of n-type pbTe/$pb_{1-x}Eu_xTe$ quantum wells, J. Phys. Sciences, (1) : 100-105.
12. Weidenkaffa,A.; Roberta,R.; Aguirrea,M.; Bochera,L.; Lippertb,T.and Canulescu,S. (2008) Development of thermoelectric oxides for renewable energy conversion technologies, Renewable Energy, 33:342–347.
13. Dresselhaus,M.S.; Chen,G.; Tang,M.Y.; Yang,R.; Lee,H.; Wang,D.; Ren,Z.; Fleurial,J-P.and Gogna,P. (2007) New Directions for Low-Dimensional Thermoelectric Materials, Adv. Mater. 19:1–12.
14. Han,S.W.; Hasan,M.A.; Kim,J.Y.; Lee,H.W.; Lee,K.H.and Kim,O.J. (2005) Multi-physics analysis for the design and development of micro-thermoelectric coolers, KINTEX, Gyeonggi-Do, Korea, ICCAS.
15. Casati,G.; Mejia-Monasterio,C.and Prosen,T. (2008) Increasing thermoelectric efficiency towards the Carnot limit, cond-mat. stat-mech, pp. 1-4.
16. Singh,R.; Bian,Z.; Shakouri,A.; Zeng,G.; Bahk,J-H.; Bowers,J.E.; Zide,J.M.O.and Gossard,A.C. (2009) Direct measurement of thin-film thermoelectric figure of merit, Appl. Phys. Lett. 94, 1-3.
17. Shakouri,A. (2005) Thermoelectric, thermionic and thermophotovoltaic energy conversion, Int. Conference on Thermoelectrics, IEEE, p. 492.
18. Sur,I.; Casian,A.and Balandin,A. (2004) Electronic thermal conductivity and thermoelectric figure of merit of *n*-type PbTe/$Pb_{1-x}Eu_xTe$ quantum wells, Phys. Rev. B 69, pp. 1-7.
19. Koga,T.; Sun,X.; Cronin,S.B.; Dresselhaus,M.S.; Wang,K.L.and Chen,G. (1997)Models for low-dimensional thermoelectricity, J. Computer-Aided Materials Design, 4:175-182.
20. Khitun,A.; Balandin,A.; Wang,K.L.and Chen,G. (2000) Enhancement of the thermoelectric figure of merit of $Si_{1-x}Ge_x$ quantum wires due to spatial confinement of acoustic phonons, Physica, E8, pp.13-18.
21. Chen,G.; Dresselhaus,M.S.; Dresselhaus,G.; Fleurial,J.P.and Caillat,T. (2003) Recent developments in thermo-electric materials, Int. Materials Reviews, 48(1): 1-22.
22. Goussev,A.and Bandyopadhyay,S. (2003) Universal negative differential resistance in one-dimensional resistors, Phys. Lett. A 309: 240–247.
23. Bejenari,I.and Kantser,V. (2008) Thermoelectric properties of bismuth telluride nanowires in the constant relaxation-time approximation, Phys. Rev. B 78, 115322-1-12.

IBN AL- HAITHAM J. FOR PURE & APPL. SCI. VOL.23 (3) 2010

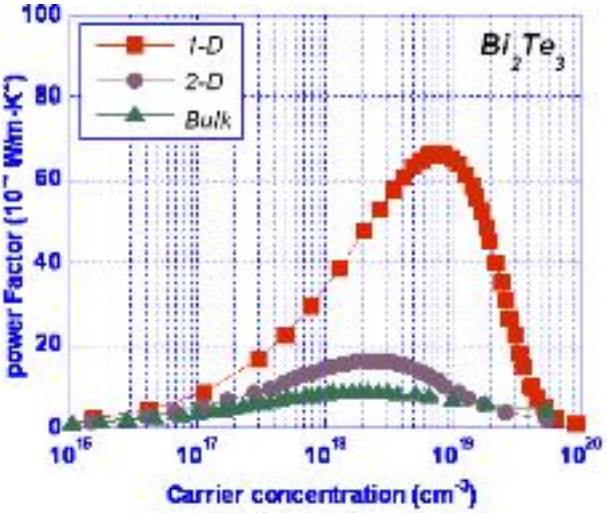
1-D
2-D
Bulk
Bi_2Te_3
power Factor (10^{-4} W/m-K^2)
Carrier concentration (cm^{-3})

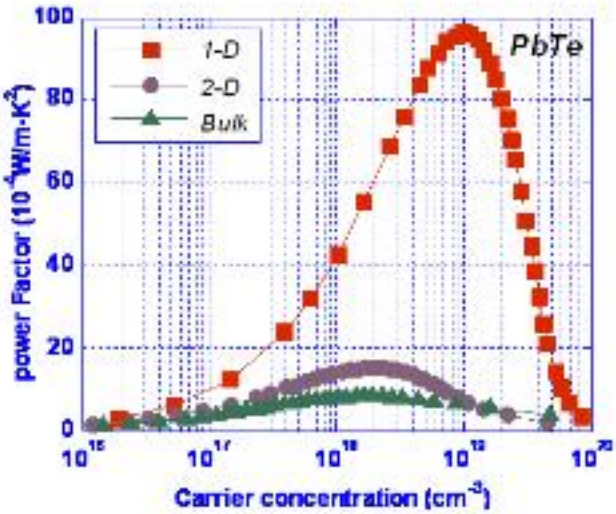
1-D
2-D
Bulk
PbTe
power Factor (10^{-4}W/m-K^2)
Carrier concentration (cm^{-3})

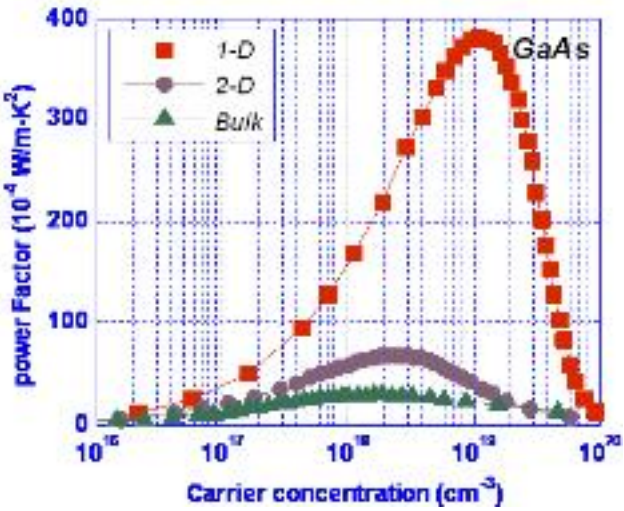
1-D
2-D
Bulk
GaAs
power Factor (10^{-4} W/m-K^2)
Carrier concentration (cm^{-3})

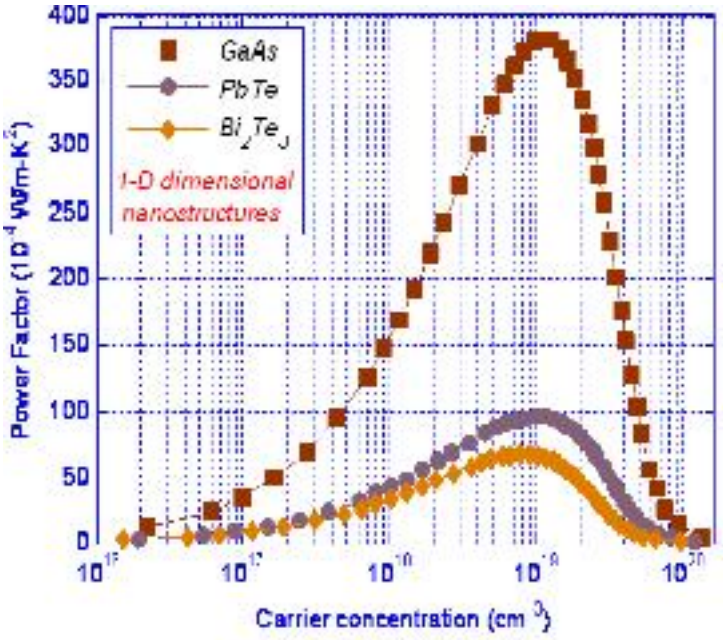

nparison of the ors predictions n-type Bi_2Te_3, GaAs for a 20Å re as a function ncentration

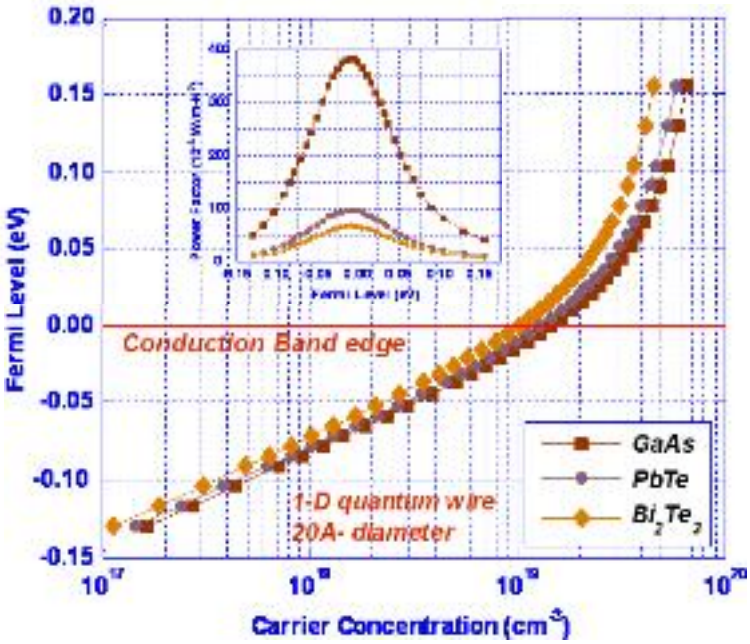

for a 1-D quantum wire. The inset shows the variation of PF with Fermi level at 20Å diameter

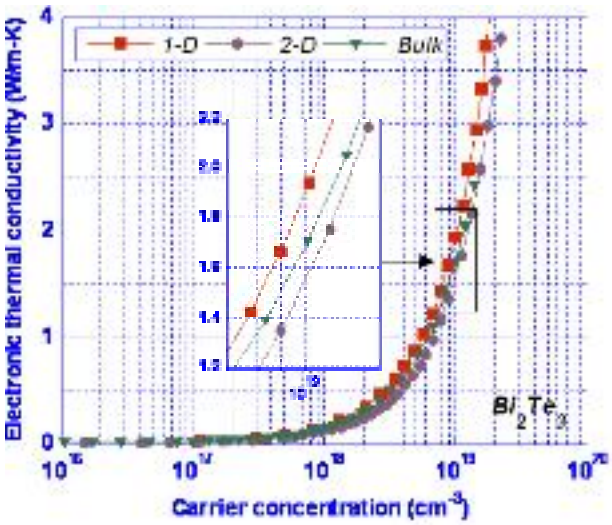

Fig.(4): Electronic thermal conductivity κ_e of the *n*-type Bi_2Te_3, PbTe and GaAs quantum-well, quantum-wire and bulk as a function of carrier concentration

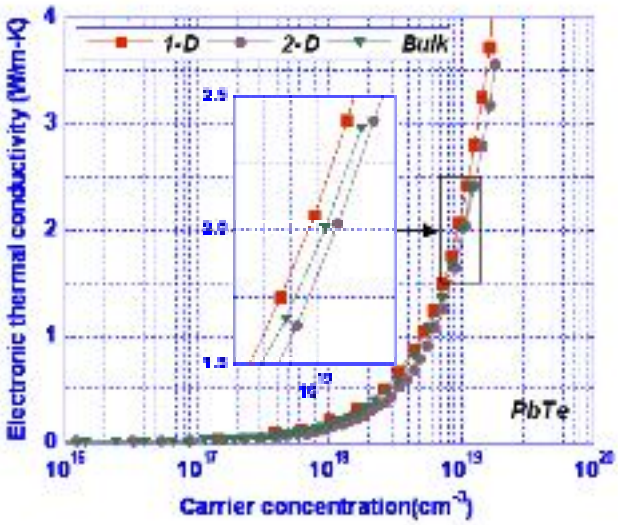

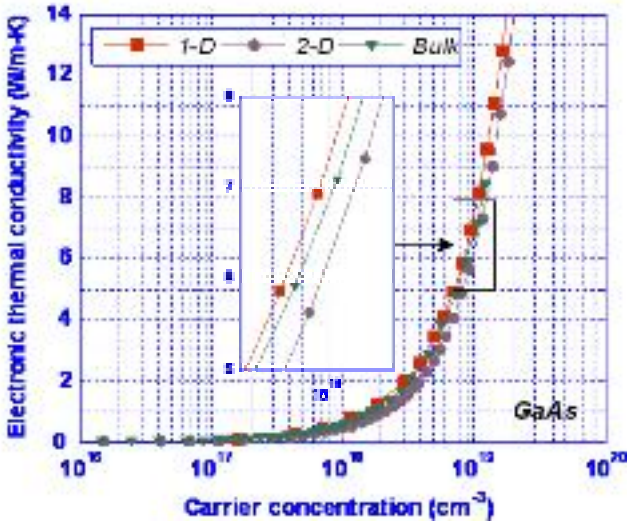

Table (1): The material parameters are used in simulations

Property	Symbol	**Bi_2Te_3** (Wurtzite) we take a six-fold valley [d]	**PbTe** (Rock-salt) we take a four-fold valley [a]	**GaAs** (Zincblende) we take a three-fold valley [f]
Phonon thermal Conductivity (Bulk)	κ_p (W/mK)	1.5 [b]	2 [a]	44 [f]
Longitudinal and Transverse effective masses	$m_{\parallel_z}^{w}/m_o$ $m_{\perp}^{w}/m_o$	mx=0.021 [d] my=0.081 [d] mz=0.32 [d]	mx=my= 0.034 [c] mz=0.35 [c]	mx= my=0.043 [g] mz=0.22 [g]
Electron bulk mobility	μ (m^2/Vs)	0.15 [h]	0.17 [e]	0.6 [g]
Dimensionless bulk Figure of Merit	ZT	0.52 [e]	0.36 [e]	0.0085 [f]

[a] Data taken from Ref. 4.

[b] Data taken from Ref. 14.

[c] Data taken from Ref. 18.

[d] Data taken from Ref. 23.

[e] Broido,D.A.; Reinecke,T.L.; **Thermoelectric transport in quantum well superlattices**, (1997) Appl. Phys. Lett., Vol. 70, No.21, pp. 2834-6.

[f] Koga,T.; Sun,X.; Cronin,S.B.; Dresselhaus,M.S.; **Carrier pocket engineering to design superior thermo-electric materials using GaAs/AlAs superlattices**, (1998) Applied physics letters Vol.73, No.20, pp. 2950-2.

[g] Sze,S. M.; Kwok,K.Ng.; **Physics of Semiconductor Devices**, 3rd Edition, John Wiley & Sons, Inc. (2007) (Appendix F & p.549).

[h] Balandin,A.; Wang,K.L.; **Effect of phonon confinement on the thermoelectric figure of merit of quantum wells**, (1998), j. Appl. Phys. Vol.84, No.11, pp. 6149-53.

Table (2): Calculated dimensionless figure of merit for the three materials nanowire (20Å dimeter) and nanowell (20Å thickness).

Material	$Z_{2D}T$	$Z_{1D}T$
Bi_2Te_3	1.1654	3.3833
PbTe	0.2022	1.0425
GaAs	0.0448	0.2397